Spectrochimica Acta Part A: Molecular and Biomolecular Spectroscopy 113 (2013) 314–324

Contents lists available at SciVerse ScienceDirect

Spectrochimica Acta Part A: Molecular and Biomolecular Spectroscopy

journal homepage: www.elsevier.com/locate/saa

Phenylazoindole dyes – Part I: The syntheses, characterizations, crystal structures, quantum chemical calculations and antimicrobial properties

Zeynel Seferoğlu [a,*], Ergin Yalçın [a], Banu Babür [a], Nurgül Seferoğlu [b], Tuncer Hökelek [c], Ebru Yılmaz [d], Ertan Şahin [e]

[a] Gazi University, Department of Chemistry, 06500 Ankara, Turkey
[b] Gazi University, Advanced Technologies, 06500 Ankara, Turkey
[c] Hacettepe University, Department of Physics, 06800 Ankara, Turkey
[d] Gazi University, Vocational School of Health Sciences, 06830 Ankara, Turkey
[e] Atatürk University, Department of Chemistry, Erzurum, Turkey

HIGHLIGHTS

- Phenylazoindole based new organic dyes have been synthesized and characterized.
- The most stable tautomeric form of the dyes have been determined easily with using model compounds in solution.
- The quantum chemical calculations results showed that the azo tautomer is dominant tautomeric form.

GRAPHICAL ABSTRACT

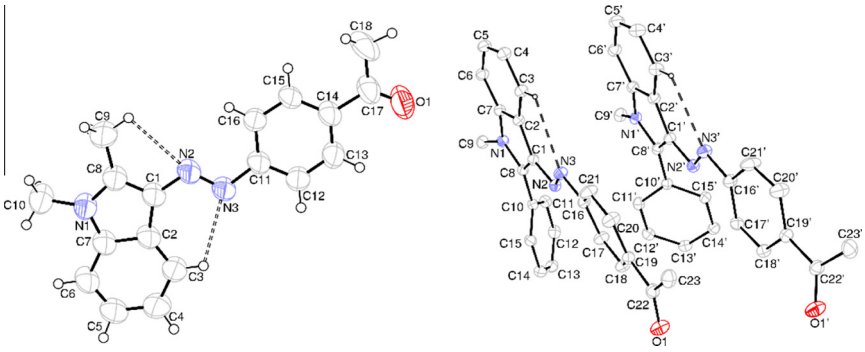

ARTICLE INFO

Article history:
Received 10 October 2012
Received in revised form 1 March 2013
Accepted 24 April 2013
Available online 14 May 2013

Keywords:
Phenylazoindole dye
Azo–hydrazone tautomer
Crystal structure
DFT calculations
Antimicrobial activity

ABSTRACT

In this study, the synthesis of four new phenylazo indole dyes (dye 1–4) were carried out by diazotization of 4-aminoacetophenone and coupling with various 2- and 1,2-disubstituted indole derivatives. The dyes were characterized by UV–vis, FT-IR, ^{1}H NMR, HRMS and X-ray single crystal diffraction methods. Azo–hydrazone tautomeric bahavior of the dyes in different solvents (DMSO, methanol, acetic acid and chloroform) was investigated by using ^{1}H NMR and UV–vis results. The experimental results were compared with the corresponding calculated values. The results of experimental data and theoretical calculations showed that the azo tautomer is more stable than hydrazone tautomer. In addition to this, the antimicrobial activity of the dyes was also evaluated.

Published by Elsevier B.V.

Introduction

Azo compounds, with two phenyl or hetaryl rings separated by an azo (N=N) bond, are versatile molecules and have been used as dyes and pigments for a long time in research areas both fundamental and application [1]. It has been known for many years that the azo compounds are the most widely used class of dyes, due to their versatile applications in various fields such as the dyeing of textile fibers, the coloring of different materials, colored plastics and polymers, biological–medicinal studies, as chemosensor and advanced applications in organic synthesis [2–9]. They are also used in the fields of nonlinear optics and optical data storage [10–12]. Their optical properties depend on not only the

* Corresponding author. Tel.: +90 312 2021525; fax: +90 312 2122279.
E-mail address: znseferoglu@gazi.edu.tr (Z. Seferoğlu).

1386-1425/$ - see front matter Published by Elsevier B.V.
http://dx.doi.org/10.1016/j.saa.2013.04.081

spectroscopic properties of the molecules, but also their crystallographic arrangements [13,14]. Carbocyclic diazo components have been used extensively in the preparation of disperse dyes. These dyes are also characterized by having generally excellent brightness and high extinction coefficients and also many carbocyclic diazo components have been current potential dyestuffs in dye industry. On the other hand, many azo dye breakdown products are carcinogenic, toxic and mutagenic for life [15]. However, the antimicrobial activity of some azo dyes has been reported previously [16–19].

Tautomerism is quite interesting from a theoretical viewpoint and it is also important from a practical standpoint because the two tautomers have different technical properties [20]. Azo–hydrazone, annular tautomerism and other tautomeric structures that exist in the azo compounds have been extensively attempted by several researchers to recognize their exact geometrical structures and stability in gas phase (theoretically) and in the presence of solvent molecules. The azo/hydrazone tautomerism of hydroxy and amino substituted azo compounds has been intensively studied but enamine type azo compounds have not been investigated deeply. Therefore, tautomeric equilibria of phenylazo dyes prepared from enamine-type coupling components need to be considered.

The aim of this study is to determine the most stable tautomeric form of some new phenylazoindole dyes in solution and solid state. For this purpose, four compounds (dyes 1–4) were synthesized for the first time and characterized by using the spectroscopic techniques (UV–vis, FT-IR, ^{1}H NMR, HRMS). The crystalline and molecular structures of dyes 2 and 4 obtained by X-ray diffraction analysis were evaluated. In addition, the geometry optimizations, the stabilities and maximum absorption wavelengths of the dyes in gas phase and in solution state and ^{1}H NMR chemical shifts of the dyes 1–4 were discussed. Also, antimicrobial activities of the dyes were investigated.

Experimental

Material and methods

The chemicals used in the synthesis of all compounds were from the Aldrich Chemical Company and used without further purification. The solvents were used of spectroscopic grade. IR spectra were recorded on a Mattson 1000 FT-IR spectrophotometer in KBr (ν are in cm^{-1}). H NMR spectra were recorded on a Bruker-Spectrospin Avance DPX 400 Ultra-Shield in DMSO-d_6. Chemical shifts are expressed in δ units (ppm). Ultraviolet–visible (UV–vis) absorption spectra were recorded on Analytik Jena Specord 200 spectrophotometer at the wavelength of maximum absorption (λ_{max}, in nm) in the solvents specified. The methanolic solutions of the dyes were examined, when was added 0.1 mL KOH (0.1 M) or 0.1 mL HCl to 1 mL of the dye solutions. Mass spectra were recorded on Waters-LCT-Premier-XE-LTOF (TOF-MS) instruments; in m/z (rel.%). The X-ray data were recorded in the Department of Chemistry, Atatürk University, Erzurum, Turkey.

Microorganisms

The antimicrobial activities of the synthesized dyes (1–4) were determined by the well-diffusion method [21]. 2 *Staphylococus aureus*, 2 *S. saprophyticus*, 1 *Listeria monocytogenes*, 1 *L. innocua* (Gram Positive), 4 *Pseudomonas aeruginosa*, 2 *P. putida*, 5 *Escherichia coli*, 2 *Klebsiella pneumoniae*, 2 *Enterobacter sakazakii* (Gram Negative), and 2 *Candida albicans*, 1 *Candida tropicalis* (fungus) were used to investigate the antibacterial and antifungal activities of synthesized dyes. *Staphylococus aureus*, *S. saprophyticus*, *Listeria monocytogenes*, *L. innocua*, *Pseudomonas aeruginosa*, *P. putida*, *Escherichia coli*, *Klebsiella pneumoniae*, *Enterobacter sakazakii* liquid cultures were prepared in brain heart infusion broth for their antimicrobial activity tests and *Candida albicans*, *Candida tropicalis* were prepared in Sabouraud dextrose broth for its antifungal activity tests. The dyes were dissolved in DMSO at concentrations of 10 mg mL^{-1} using a Millipore membrane filter (0.45 mL, Millipore, USA). Antimicrobial activity of DMSO against the test organisms was also investigated, but was found to have no antimicrobial activity against any of the organisms. Approximately 1 cm^3 of a 24 h broth culture containing 10^6 cfu cm^{-3} was placed in sterile Petri dishes. Moltent nutrient agar (15 cm^3) kept at 45 °C was then poured into the Petri dishes and allowed to solidify. Six milimeter diameter holes were then punched carefully using a sterile cork borer and completely filled with the test solutions. The plates were incubated for 24 h at 37 °C. After 24 h., the inhibition zone that appeared around the holes in each plate was measured. Sulbactam ampicillin (SAM), Gentamisin (CN), Sulfamethoxazole Trimethoprim (SXT) and Miconazole (MCZ) were screened under similar conditions as a reference Standard.

In this work, 2 *Staphylococus aureus*, 2 *S. saprophyticus*, 1 *Listeria monocytogenes*, 1 *L. innocua* (Gram Positive), 4 *Pseudomonas aeruginosa*, 2 *P. putida*, 5 *Escherichia coli*, 2 *Klebsiella pneumoniae*, 2 *Enterobacter sakazakii* (Gram Negative), 2 *Candida albicans*, 1 *Candida tropicalis* (Yeast) were used to investigate the antibacteriological and antifungal activities of synthesized dyes 1–4. Used microorganisms were isolated from Gazi University, Faculty of Science and Arts, Department of Biology.

Preparation of dyes (1–4)

Various carbocyclic amines can be diazotized with HCl and $NaNO_2$. A typical procedure of diazotizing and coupling is that described below used for 4-aminoacetophenone and 2-methylindole; all other compounds were prepared in a similar manner. The yields of the dyes are in the range of 78–90%. The obtained compounds were purified by crystallization using ethanol and then analyzed.

Preparation of (E)-1-(4-((2-methyl-1H-indol-3-yl)diazenyl)phenyl)ethanone (1)

4-Aminoacetophenone (0.27 g, 2 mmol) was dissolved in concentrated HCl (1.5 mL, 36 % (w/w)) and water (4 mL). The solution was cooled in an ice–salt bath and a cold solution of $NaNO_2$ (0.15 g, 2 mmol) in water (3.0 mL) was added dropwise with stirring. The mixture was stirred for an additional 1 h. at 273 K. Excess nitrous acid was destroyed by the addition of urea. The resulting diazonium salt was cooled in a salt/ice mixture. 2-Methylindole (0.26 g, 2.0 mmol) was dissolved in a mixture of acetic acid and propionic acid solution (3:1, 8 mL) and cooled in an ice bath. Then, cold diazonium solution was added to this cooled solution by stirring in a dropwise manner. The solution was stirred at 273–278 K for 1 h. The pH of the reaction mixture was maintained at 4–6 by the simultaneous addition of saturated sodium carbonate solution. The mixture was stirred for a further 1 h. at room temperature. The resulting solid was filtered, washed with cold water and dried. Recrystallization from ethanol gave orange crystals (MW: 277 g/mol, yield: 0.25 g, 90%; m.p.: 246 °C) FT-IR (KBr) ν_{max}: 3236 (NH indole), 3067 (aromatic C—H), 2910 (aliphatic C—H), 1661 (C=O), 1593 (C=C) cm^{-1}; ^{1}H NMR (DMSO-d_6): δ 12.20 (brs, NH indole), 8.39 (d, 1H), 8.11 (d, 2H), 7.90 (d, 2H), 7.41 (d, 1H), 7.20 (m, 2H), 2.80 (s, 3H), 2.68 (s, 3H). HRMS (m/z): $(M+H)^+$ calcd for $C_{17}H_{15}N_3O$ 278.1293; found, 278.1293.

(E)-1-(4-((1,2-dimethyl-1H-indol-3-yl)diazenyl)phenyl)ethanone (2)

The dye was obtained from 4-aminoacetophenone and 1,2-dimethylindole as orange crystals (MW: 291 g/mol, $C_{18}H_{17}N_3O$ yield: 0.26 g, 88%; m.p.: 136 °C) ν_{max}: 3050 (aromatic C—H),

2910, 2870 (aliphatic C—H), 1672 (C=O), 1600, 1530 (C=C) cm^{-1}; ^1H NMR (DMSO-d_6): δ 8.43 (d, 1H), 8.10 (d, 2H), 7.90 (d, 2H), 7.58 (d, 1H), 7.30 (m, 2H), 3.81 (s, 3H, —NCH_3), 2.80 (s, 3H), 2.61 (s, 3H). HRMS (m/z): $(M+H)^+$ calcd for $C_{17}H_{15}N_3O$ 292.1450; found, 292.1446.

(E)-1-(4-((2-phenyl-1H-indol-3-yl)diazenyl)phenyl)ethanone (3)

The dye was obtained from 4-aminoacetophenone and 2-phenylindole as orange crystals (MW: 339 g/mol, yield: 0.28 g, 83%; m.p.: 227 °C) ν_{max}: 3263 (NH indole), 3063 (aromatic C—H), 2928 (aliphatic C—H), 1656 (C=O), 1594 (C=C) cm^{-1}; ^1H NMR (DMSO-d_6): δ 12.52 (brs, NH indole), 8.51 (d, 1H), 8.21 (d, 2H), 8.12 (d, 2H), 7.90 (d, 2H), 7.64 (m, 2H), 7.51 (m, 2H), 7.30 (m, 2H), 2.65 (s, 3H). HRMS (m/z): $(M+H)^+$ calcd for $C_{22}H_{17}N_3O$ 340.1442; found, 340.1438.

(E)-1-(4-((1-methyl-2-phenyl-1H-indol-3-yl)diazenyl)phenyl)ethanone (4)

The dye was obtained from 4-aminoacetophenone and 1-methyl-2-phenylindole as red crystals (MW: 353 g/mol, yield: 0.27 g, 77%; m.p.: 279 °C) ν_{max}: 3028 (aromatic C—H), 2924 (aliphatic C—H), 1674 (C=O), 1593 (C=C) cm^{-1}; ^1H NMR (DMSO-d_6): δ 8.52 (d, 1H), 8.08 (d, 2H), 7.72–7.80 (m, 6H), 7.60 (d, 2H), 7.40 (m, 2H), 3.88 (s, 3H, —NCH_3), 2.62 (s, 3H). HRMS (m/z): $(M+H)^+$ calcd for $C_{23}H_{19}N_3O$ 354.1606; found, 354.1600.

Computational study

All calculations were performed with the aid of the GAUSSIAN 09 software [22]. Becke's three-parameter exact-exchange functional (B3), combined with the gradient-corrected correlation functional of Lee–Yang–Parr (LYP) of the density functional theory methods (B3LYP) [23] were used for geometry optimizations. 6-311+g(d,p) Basis set was used in all optimization calculations. The optimized structures were characterized as true minima by vibrational frequency calculations. The optimized structure in gas phase was used for NMR calculations. The calculations of ^1H NMR chemical shielding in DMSO for all dyes were performed using GIAO/DFT [24,25] method at 6-311+g(d,p) basis sets.

The ^1H-shieldings were converted into the predicted chemical shifts using δ_{TMS} values for shielding constant of tetramethylsilane hydrogens calculated at the same level of theory according to the general expression $\delta_{Cal} = \delta_{TMS} - \delta$.

The electronic spectra of the compounds in azo form were also obtained in the framework of TD-DFT calculations with B3LYP using 6-311g(d,p) basis set. In these calculations, different solvents was used to evaluate of the solvent effects on maximum absorption wavelength for each molecule.

Crystallography

The X-ray diffraction data collections were performed on a Rigaku R-AXIS RAPID-S diffractometer using Mo Kα radiation (λ = 0.71073 Å) at T = 298 K. Absorption corrections by multi-scan [26] were applied. The structures were analyzed using a combination of direct and difference Fourier methods provided by the SHELXS97 [27] and were refined as full-matrix least squares against F^2 using all data by the SHELXL97 [27] computer programs; all non-hydrogen atoms were refined anisotropically. H atoms were positioned geometrically at distances of 0.93 (CH) and 0.96 Å (CH_3) from the parent C atoms; a riding model was used during the refinement processes and the U_{iso}(H) values were constrained to be xU_{eq}(carrier atom), where x = 1.5 for methyl H, and x = 1.2 for aromatic H atoms. Crystal data and details of the structure determinations for dyes 2 and 4 are summarized in Table 1.

Results and discussion

The phenylazoindole dyes (1–4) were prepared by coupling 2-methylindole, 1,2-dimethylindole, 2-phenylindole and 1-methyl-2-phenyl indole with diazotized 4-aminoacetophenon in dilute hydrochloric acid (Scheme 1). The dyes (1–4) were obtained generally in excellent yields (90–77%); the structure of these dyes were verified by spectroscopic methods (FT-IR, Mass and ^1H NMR). Physical and spectral data of dyes prepared are given in experimental section. The dyes prepared from 2-methylindole (dye 1) and 2-phenylindole (dye 3) may exist in two possible tautomeric forms, namely azo form A and hydrazone form B, as depicted in Scheme 2. The protonation and deprotonation of the two tautomers lead to the common anion C and cation D.

The infrared spectra of dyes 1 and 3 (in KBr) showed weak and broad band in the 3236 and 3263 cm^{-1}, due to the —NH band of the indole rings. ^1H NMR spectra of the dyes showed the —NH peaks in the range of 12.52–12.20 ppm in DMSO-d_6. These results suggest that the dyes 1 and 3 are predominantly exist in the azo form in the solid state and into solution (DMSO).

Table 1
Crystal data and details of the structure determinations for dyes 2 and 4.

Empirical formula	$C_{18}H_{17}N_3O$ (**2**)	$C_{23}H_{19}N_3O$ (**4**)
Formula weight	291.35	353.41
Crystal dimensions (mm)	0.20 × 0.20 × 0.10	0.35 × 0.25 × 0.20
Temperature (K)	294	294
Crystal system	Monoclinic	Monoclinic
Space group	$P2_1/n$	$P2_1/c$
a (Å)	9.8216(4)	10.2842(2)
b (Å)	11.7784(3)	17.5313(3)
c (Å)	13.5508(4)	21.1442(5)
β (°)	100.692(2)	101.282(3)
Volume (Å^3)	1540.38(9)	3738.53(14)
Z	4	8
D_{calc} (g cm^{-3})	1.256	1.256
$2\theta_{max}$ (°)	52.8	56.0
μ (mm^{-1})	0.08	0.08
No. of reflections measured	31,380	102,670
No. of reflections observed [$I > 2\Delta(I)$]	2296	4273
No. of variables	3142	11,432
R/R_w values	0.0698/0.1311	0.073/0.223
Color/shape	Orange/plate	Red/block
Maximum shift in final cycles	0.000	0.000
Largest diffraction peak and hole (e Å^{-3})	0.400 and −0.290	0.150 and −0.250

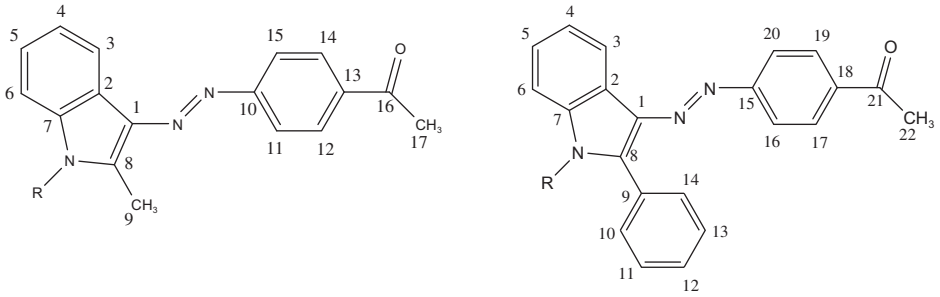

R= H (dye 1); R= CH_3 (dye 2)

(a)

R= H (dye 3); R= CH_3 (dye 4)

(b)

Scheme 1. Structures of dyes.

Solvent effects on absorption spectra of the dyes

The azo dyes are the most important commercial coloring materials. Thus, determination of the dominant tautomeric structure of azo dyes in different solutions which has different potential tautomeric structures, is quite important. In this work, the absorption spectra of phenylazoindole dyes (1–4) were recorded over the range of λ between 300 and 700 nm using a variety of solvents in concentrations 10^{-6}–10^{-8} M. In order to understand the most stable tautomeric form of the prepared dyes in solution, the compounds (dyes 2 and 4) has been used as model compound for dyes 1 and 3. The used solvents have different dielectric constants (ε), i.e. DMSO (ε, 46.45), methanol (ε, 32.66), acetic acid (ε, 6.17) and chloroform (ε, 4.81). The results are given in Table 2.

The absorption maxima of the dyes were found to be independent of the solution phase and did not have a correlation with the dielectric constants of the solvents. The model compounds (2 and 4) exist in the solely azo form and their absorption maxima in different solvents were found to exhibit little solvent dependence.

The absorption curves of dyes 1–4 in various solvents are shown in Fig. 1. When λ_{max} values of dye 1 are compared with its corresponding model compound (dye 2), dye 1 is in favor of the predominantly azo form in all solvents used (Fig. 1a and b). The small hypsochromic and bathochromic shifts in λ_{max} of these dyes in used solvents are due to solute–solvent interactions. Dye 1 showed absorption maxima at 409 nm in acetic acid, 409 nm in DMSO, 402 nm in methanol, 397 nm in chloroform (Table 2). The similar absorption maximum values were observed for dye 2 (e.g. 414 nm in acetic acid, 413 nm in DMSO, 406 nm in methanol, and 408 nm in chloroform). The same trend has been seen in the dyes 3 and 4 (Fig. 1c and d, Table 2).

The synthesized phenylazoindole dyes theoretically may be involved in azo–hydrazone tautomers (Scheme 2). Thus, the role of the azo–hydrazone tautomerism in relation to the visible absorption spectra and solvatochromic behavior of the dyes have also been investigated. The visible absorption spectra of the prepared dyes showed one absorption maximum in all solvents used, with the exception of dye 3 in DMSO (Fig. 1c). Two absorption maxima may indicate the presence of an azo–hydrazone tautomeric

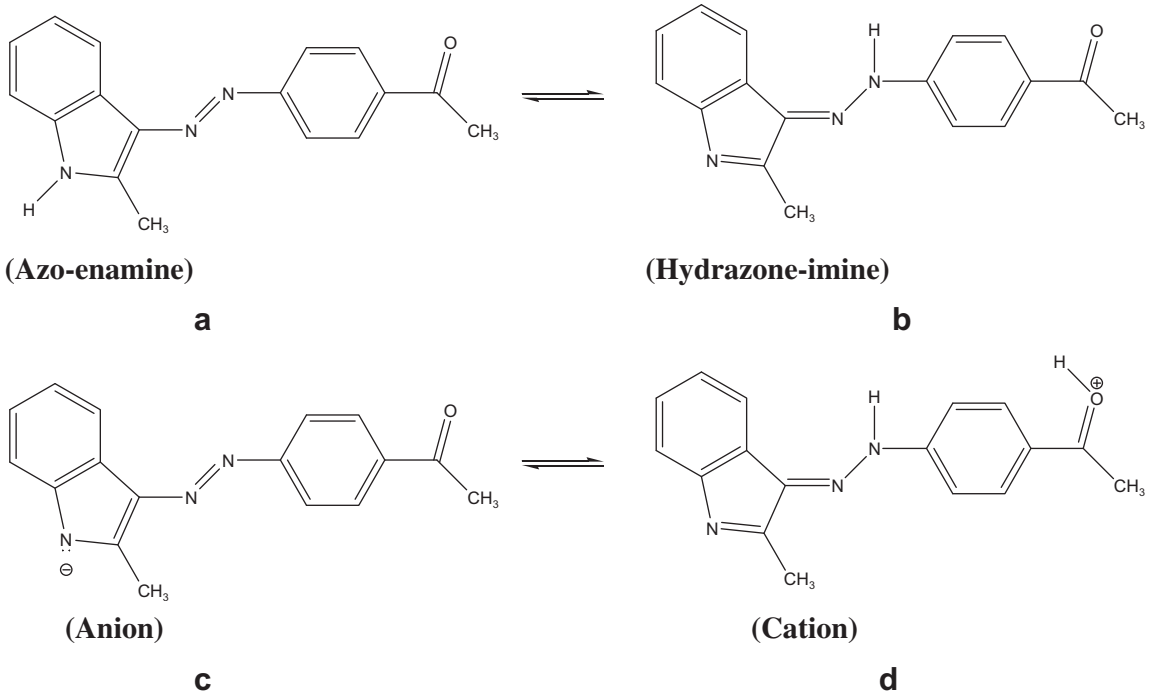

(Azo-enamine) **(Hydrazone-imine)**

a **b**

(Anion) **(Cation)**

c **d**

Scheme 2. Tautomeric forms of dye 1.

Table 2
Absorption maxima of the dyes in solvent and acidic/basic solution.

λ_{max} (nm)								
	DMSO	DMSO + piperidine	Methanol	Methanol + KOH	Methanol + HCl	A.Acid	Chloroform	Chloroform + piperidine
Dye 1	409	409,515	402	401	440	409	397	402
Dye 2	413	412	408	406	440	414	408	408
Dye 3	430,530	534	422	421	445	421	417	419
Dye 4	417	417	402	401	440	414	413	412

equilibrium or equilibrium between one of the tautomeric forms and an anionic form.

The visible absorption spectra of the dyes prepared indicated that 1-methyl-2-phenyl substituted dyes (3 and 4) generally absorp bathochromically compared with the 1,2-dimethyl substituted dyes (1 and 2) in all solvents used (Table 2). The λ_{max} values of dye 1 showed bathochromic shifts in all solvents when compared with dye 3 (for dye 1, $\Delta\lambda_{max}$ values are 21 nm in DMSO, 20 nm in methanol, 12 nm in acetic acid and 20 nm in chloroform relative to $\Delta\lambda_{max}$ of 3 in the same solvents). Presumably, the resonance effect enhanced by an π-electron-rich phenyl group is more favored than the slightly strong field effect of a methyl group. The similar increasing values of $\Delta\lambda_{max}$ results did not observe for the model compounds. For dye 2, $\Delta\lambda_{max}$ values are 4 nm in DMSO, 4 nm in methanol, 0 nm in acetic acid and 5 nm in chloroform relative to λ_{max} of 4 in the same solvents.

The effects of acid or base on the absorption maxima of the dyes in solution were investigated and the results were shown in Table 2. The absorption maximum of dye 1 in DMSO was quite sensitive to the addition of piperidine, with the exceptions of the model compounds (2 and 4) (Fig. 2a). λ_{max} of dyes 1 and 3 showed large bathochromic shifts when a small amount of piperidine was added to each of the solutions in DMSO. For dye 1, $\Delta\lambda_{max}$ is 25 nm in DMSO + piperidine relative to DMSO. Dye 3 has two absorption maxima in DMSO (Fig. 2b). When a small amount of piperidine was added, the absorption band of this dye significantly changed and showed one dominant absorption maxima in long wavelength. It indicated that dye 3 exists in only anionic form (C) in basic DMSO

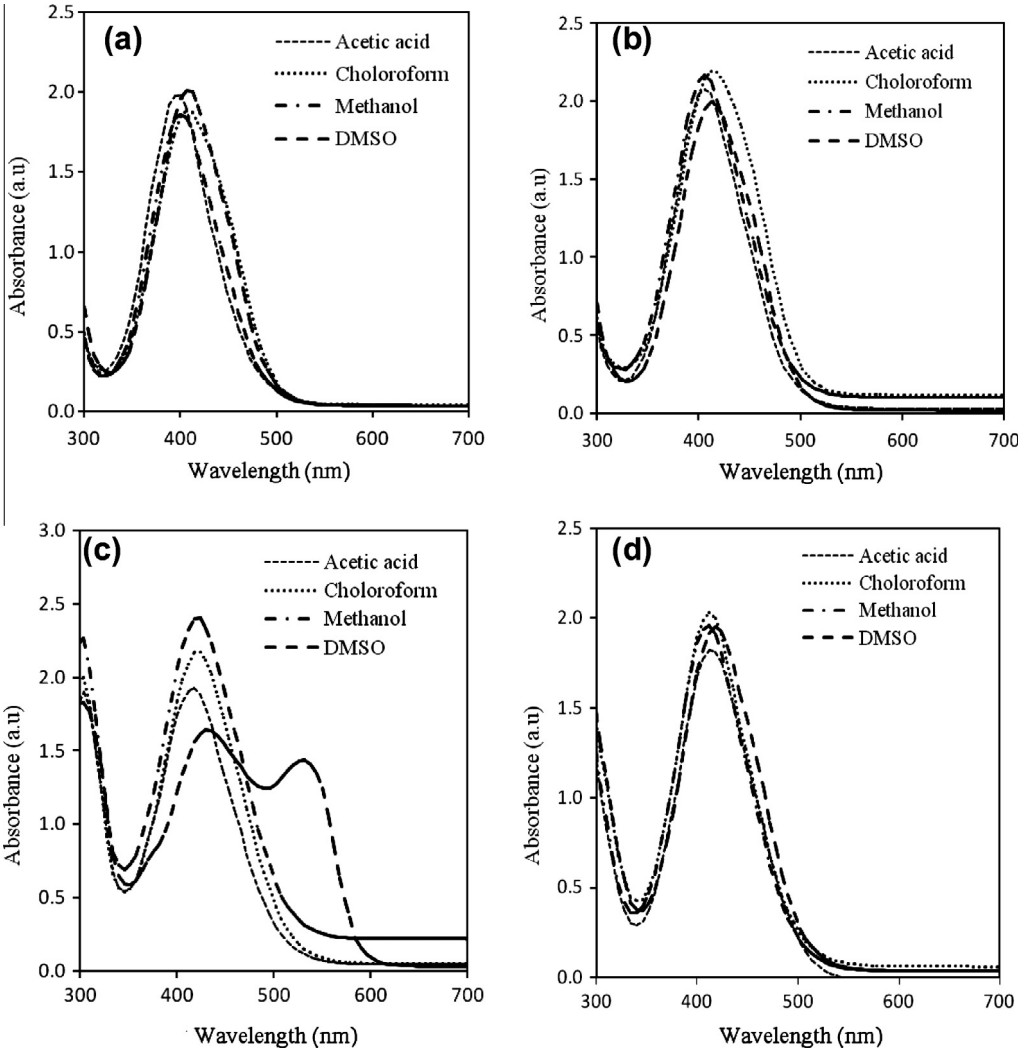

Fig. 1. Absorption spectra in various solvents for (a) dye 1, (b) dye 2, (c) dye 3, (d) dye 4.

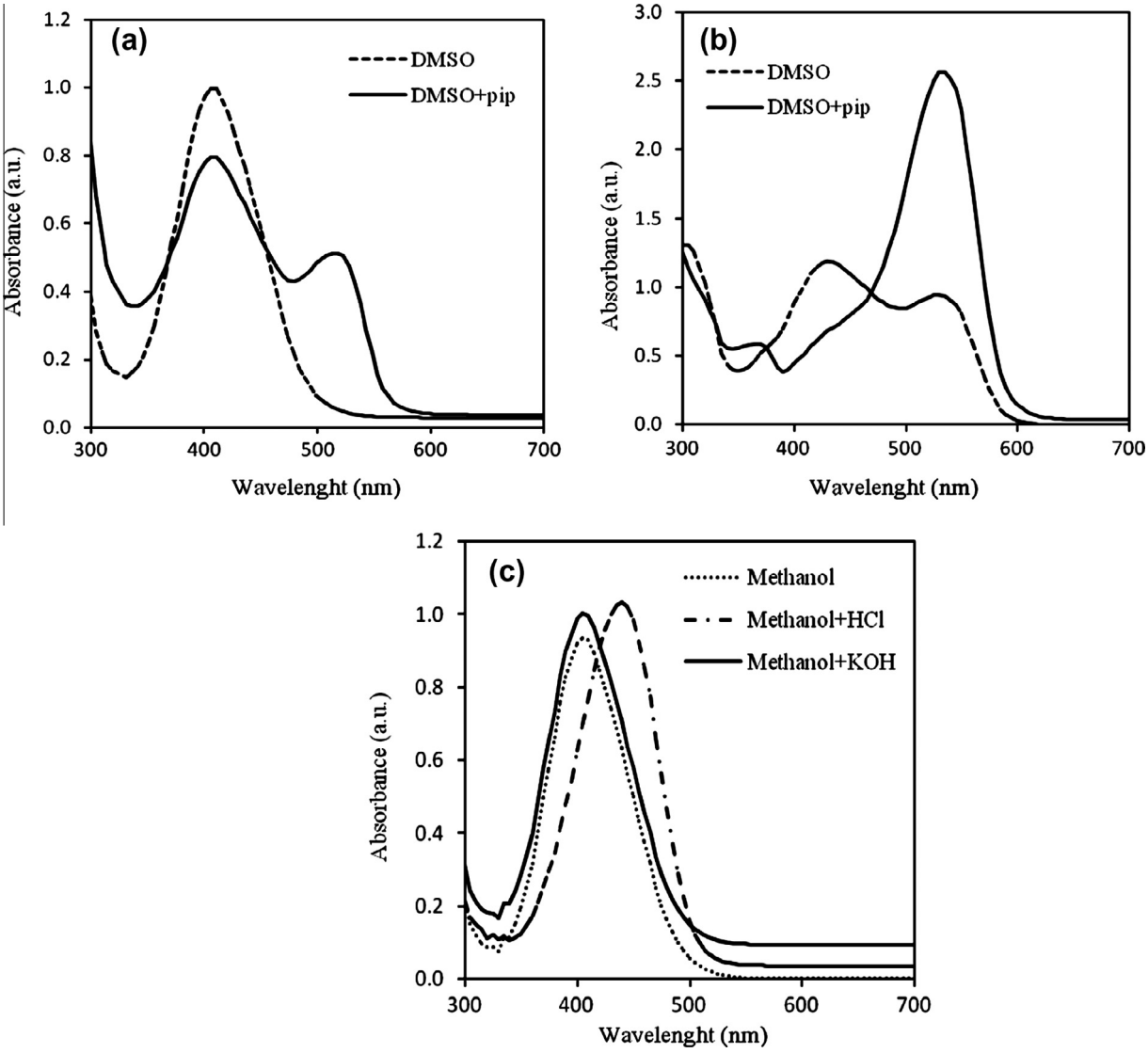

Fig. 2. Absorption spectra of (a) dye 1 in basic DMSO and DMSO solution, (b) dye 3 in basic DMSO and DMSO solution, (c) dye 1 in acidic and basic solution.

and between the tautomeric forms and anionic forms in neutral DMSO.

There was no significantly change in the spectra of the dyes when 0.1 M KOH was added to the methanolic solutions of the dyes. However, when a small amount of 0.1 M HCl was added to the methanolic solutions of the dyes the λ_{max} values showed large bathochromic shifts and also only one absorption maximum was observed. This indicates that the dyes exist in the cationic form (D) in acidic methanolic solution (Fig. 2c). Spectral data for the variously substituted azo dyes show that there was a general tendency for the visible absorption band to more bathochromically in accordance with the electron acceptor–donor chromogens in the coupling and diazo component [28]. These compounds involve a migration of electron density from the donor group towards the azo group and the absorption maxima of this type of compounds were shifted longer wavelength due to stabilization of excited state has been increased. The prepared dyes that are converted cationic form via carbonyl oxygen increased electron accepting properties (Scheme 2). So, delocalization of electrons is also increased from indole to diazenyl bridge and λ_{max} values shift to the bathochromic region. For dye 2, $\Delta\lambda_{max}$ is 32 nm in methanol + HCl relative to methanol; similarly for dye 3 $\Delta\lambda_{max}$ is 38 nm in methanol + HCl relative to methanol.

Crystal structure analyses

Several times, we try to obtained suitable single crystal to determine tautomeric structures of especially dyes 1 and 3 but it can be only obtained for two molecules (dyes 2 and 4). While there was only one molecule in the asymmetric unit for dye 2 (Fig. 3), the asymmetric unit of dye 4, containing two crystallographically independent molecules, in which geometries and conformations of them are slightly different (Fig. 4). The selected bond lengths and angles for dyes 2 and 4 are given in Table 3. An examination of the deviations from the least-square planes through the individual rings showed that all of the rings are planar in dyes 2 and 4. The indole ring systems were planar, with dihedral angles of 1.49(11)° between rings A (C2—C7) and B (N1/C1/C2/C7/C8) in dye 2, and 2.48(10)° and 1.56(10)° between rings: A (C2—C7) and B (N1/C1/C2/C7/C8), A′ (C2′—C7′) and B′ (N1′/C1′/C2′/C7′/C8′) in dye 4. In the closely related compounds, 3-(4-chlorophenyldiazenyl)-1-methyl-2-phenyl-1H-indole 5 [29], *N*-{4-[(2-phenyl-1*H*-indol-3-yl)-diazenyl]phenyl} acetamide 6 [30], 5-(4-ethoxyphenyldiazenyl)-8-hydroxyquinoline 7 [31], 2-phenyl-3-(5-ethyl-1,3,4-thiadizol-2-yldiazenyl)-1*H*-indole 8 [32], ethyl[2-(2-phenyl-1*H*-indol-3-yldiazenyl)-1,3-thiazol-4-yl] acetate 9 [33], ethyl 2-{[(2-phenyl-1*H*-indol-3-yl)diazenyl]thiazol-4-yl}acetate 10 [34], 1-methyl-2-phenyl-3-(1,3,4-thiadiazol-

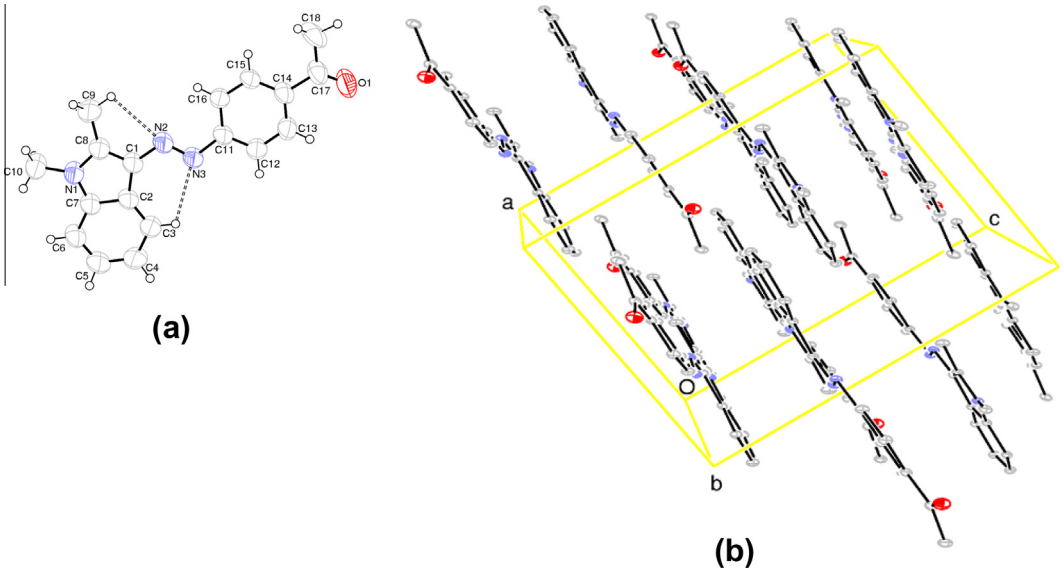

Fig. 3. (a) The molecular structure of dye 2, with the atom-numbering scheme. Displacement ellipsoids are drawn at the 50% probability level [40]. Hydrogen bonds are shown as dashed lines. (b) A partial packing diagram of dye 2 [40].

2-yldiazenyl)-1*H*-indole 11 [35], 1,2-dimethyl-3-(thiazol-2-yldiazenyl)-1*H*-indole 12 [36], 3-(5-ethyl-1,3,4-thiadiazol-2-yldia-zenyl)-1-methyl-2-phenyl-1*H*-indole 13 [37] and 3-(6-methoxybenzothiazol-2-yldiazenyl)-1-methyl-2-phenyl-1H-indole 14 [38], the observed A/B and/or A′/B′ dihedral angles were 1.56(11)° and 0.77(12)° in 5, 1.63(14)° in 6, 1.60(14)° in 7, 2.28(9)° and 1.32(11)° in 8, 0.99(10)° in 9, 0.59(7)° in 10, 4.26(7)° in 11, 0.59(12)° in 13 and 1.16(7)° in 14. The orientations of rings C (C11—C16) (in dye 2) and C (C10—C15), D (C16—C21) and C′ (C10′—C15′), D′ (C16′—C21′) (in dye 4) with respect to the indole ring systems might be described by the dihedral angles of 4.58(12)° (for dye 2) and 44.28(8)°, 12.77(7)°, 47.80(7)° and 11.94(7)° (for dye 4), respectively.

The phenyl rings are rotated around the C8—C10 and C8′—C10′ (in dye 4) bonds with the corresponding torsion angles of N1—C8—C10—C15 [−139.3(2)°] and N1′—C8′—C10′—C15′ [131.8(2)°]. The molecules of dyes 2 and 4 have *trans* geometries about the azo linkages and the torsion angles of the central —C—N=N—C— are 178.7(3)° [C1—N2—N3—C11] (for dye 2) and 178.64(19)° [C1—N2—N3—C16] and 179.8(2)° [C1′—N2′—N3′—C16′] (for dye 4).

In dye 2 (Fig. 3a), intramolecular C—H···N hydrogen bonds (Table 4) result in the formations of planar six- and five-membered rings: D (N2/N3/C1—C3/H3) and E (N2/C1/C8/C9/H9B), in which they are oriented with respect to the indole ring system at dihedral angles of 1.22(11)° and 1.49(11)°, respectively. In the crystal structure, the molecules are elongated along the *a*-axis and stacked along the *c*-axis. In dye 4, intramolecular C—H···N hydrogen bonds (Fig. 4a, Table 5) result in the formations of non-planar and planar six-membered rings: E (N2/N3/C1—C3/H3) and E′ (N2′/N3′/C1′—C3′/H3′), respectively, in which ring E′ is oriented with respect to the indole ring system at a dihedral angle of 0.42(5)°. Ring E adopts envelope conformation with atom N3 displaced by −0.180(2) Å from the plane of the other ring atoms.

In the crystal structure, intermolecular C—H···O hydrogen bonds (Table 5) link the molecules into infinite chains along the *c*-axis (Fig. 4b).

Computational analysis

The most stable structures for dyes 1–4 were obtained from the potential energy surface (PES) scan using HF/6-31G(d) method and reoptimized at the DFT level using the B3LYP/6-311+G(d,p).

The model compounds (dye 2 and 4) can be only azo form because of no intermolecular proton transfer whereas dye 1 and 3 can show the azo–hydrazone tautomerism. To compare the stability of the azo and hydrazone forms of dye 1 and dye 3, each forms of dyes are optimized in gas-phase and different solvents such as

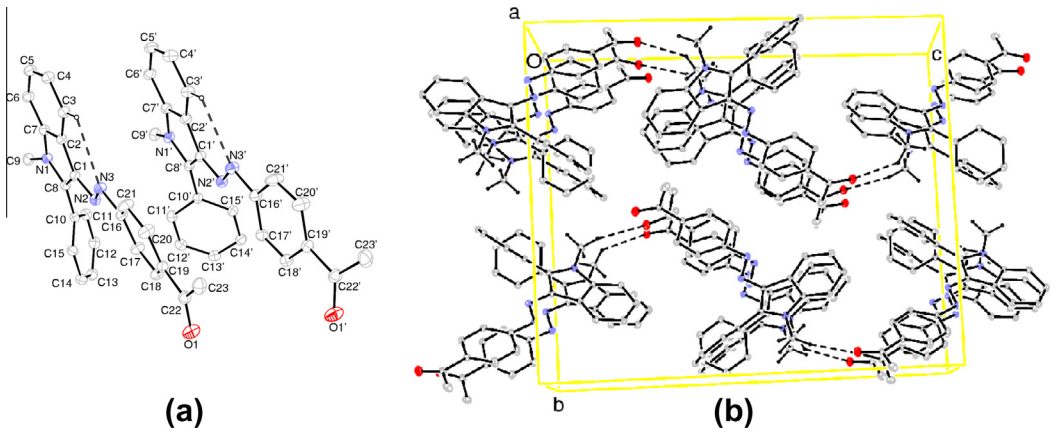

Fig. 4. (a) The molecular structure of dye 4, with the atom-numbering scheme. Displacement ellipsoids are drawn at the 50% probability level [40]. Hydrogen bonds are shown as dashed lines. (b) A partial packing diagram of dye 4 [40].

Table 3
The calculated and experimental values of selected bond lengths (Å) and angles (°) with the torsion angles (°) for dyes 1–4. For dye 4, the torsion angle values in the parenthesis are for the other conformation with the energy value −1127.63646172 a.u. and for the other of two crystallographically independent molecules obtained by X-ray crystallography.

Parameters	Dye 1	Dye 2		Parameters	Dye 3	Dye 4	
	Calc.	Calc.	Exp.		Calc.	Calc.	Exp.
Bond lengths				*Bond lengths*			
O1—C17	1.218	1.219	1.175(6)	O1—C22	1.218	1.219	1.208(3)
N1—C7	1.393	1.397	1.315(5)	N1—C7	1.389	1.394	1.392(3)
N1—C8	1.366	1.370	1.313(5)	N1—C8	1.371	1.375	1.365(3)
N2—C1	1.373	1.371	1.354(5)	N2—N3	1.268	1.268	1.275(3)
N2—N3	1.267	1.268	1.248(5)	N2—C1	1.372	1.371	1.385(3)
N3—C11	1.414	1.413	1.405(5)	N3—C16	1.413	1.414	1.418(3)
Bond angles				C8—C10	1.464	1.470	1.471(3)
C8—N1—C7	110.4	109.3	105.7 (4)	*Bond angles*			
N3—N2—C1	115.9	115.9	119.4 (4)	N3—N2—C1	115.9	116.1	113.6(2)
N2—N3—C11	114.6	114.7	116.3 (3)	N2—N3—C16	114.3	114.2	113.1(2)
N2—C1—C8	120.1	120.3	122.6 (4)	N2—C1—C2	131.5	131.9	131.7(2)
C2—C1—N2	132.3	132.2	131.2 (4)	N2—C1—C8	120.9	120.5	120.3(2)
C2—C1—C8	107.6	107.5	106.1 (4)	N1—C8—C10	120.8	123.3	122.7(2)
C1—C2—C7	106.1	105.8	104.8 (4)	C8—N1—C7	110.6	109.2	109.0(2)
Torsion angles				*Torsion angles*			
C1—N2—N3—C11	179.9	180.0	178.7(3)	C1—N2—N3—C16	178.2	−178.9(179.0)	178.64(19)(179.8(2))
N2—N3—C11—C12	179.9	180.0	175.7(4)	N1—C8—C10—C11	−32.0	50.8(−50.8)	42.6(3)(−48.6(3))
N3—N2—C1—C2	0.0	0.0	0.0(7)	N1—C8—C10—C15	147.0	−130.9(130.9)	−139.3(2)(131.8(2))
N2—C1—C8—C9	0.0	0.0	0.0(7)	N2—N3—C16—C21	170.4	−174.4(174.4)	−174.2(2)(170.0(3))
C9—C8—N1—C7	180.0	180.0	178.5(4)	N2—N3—C16—C17	−10.8	6.2(−6.2)	4.2(4)(−9.7(4))
				C8—C1—N2—N3	178.5	−179.1(179.1)	−174.3(2)(178.1(2))

Table 4
Hydrogen bond geometry (Å, °) for dye 2.

D—H···A	D—H	H···A	D···A	D—H···A
C3—H3···N3	0.93	2.55	3.016(5)	111
C9—H9B···N2	0.96	2.59	2.976(6)	104

Table 5
Hydrogen bond geometry (Å, °) for dye 4.

D—H···A	D—H	H···A	D···A	D—H···A
C3—H3···N3	0.93	2.61	3.069(3)	111
C3′—H3′···N3′	0.93	2.57	3.037(3)	111
C9—H9C···O1′^{i}	0.96	2.54	3.266(3)	133
C9′—H9D···O1^{ii}	0.96	2.55	3.457(3)	157

Symmetry code: (i) $x + 1$, $-y + ½$, $z - ½$, (ii) x, $-y + ½$, $z - ½$.

DMSO, chloroform, methanol and acetic acid. The obtained relative stability from the total energies (ΔE) and the sum of electronic and thermal free energies (ΔG) are given Table 6. The results indicate that the azo form is more stable than the hydrazone form with ΔE = 4.82 kcal/mol, ΔG = 5.11 kcal/mol for dye 1 and ΔE = 4.80 kcal/mol, ΔG = 4.25 kcal/mol for dye 3 in gas-phase. Furthermore, the relative energy values indicate that the stability of azo form of each dyes does not change with respect to the interaction of the solvent with the molecules. These results are in compatible with the experimental results indicating that dyes 1 and dye 3 are predominantly in azo form in used solvents.

The calculated and experimental values of selected bond lengths, bond angles and important torsion angles for the dyes 2 and 4 are given in Table 3. However, the values are also given for dyes 1 and 3 to compare with the corresponding model compounds, i.e. dyes 2 and 4. It is found that the optimized geometry of dye 2 were found to be consistent with the X-ray crystal structure results. C1—N2—N3—C11 torsion angle is obtained as 180.0° from the optimization and 178.7(3) from the experimental results. The optimized geometry of the dye 1 were also planar and the torsion angle C1—N2—N3—C11 is obtained as 179.9°.

For dye 4, two stable conformations were obtained as a result of PES scan with the total energy of −1127.63646170 a.u. and −1127.63646172 a.u. (Fig. 5). It has been observed that there no

Table 6
The relative energies for the azo (a) and hydrazone (h) forms of the dyes 1 and 3.

	Dye 1	ΔE^{a} (kcal/mol)	G^{b} (Hartree)	ΔG^{b} (kcal/mol)	Dye 3	ΔE^{a} (kcal/mol)	G^{b} (Hartree)	ΔG^{b} (kcal/mol)
Gas phase	a	0	−896.30314	0	a	0	−1088.036652	0
	h	4.82	−896.294992	5.11	h	4.80	−1088.029873	4.25
DMSO	a	0	−896.320768	0	a	0	−1088.053594	0
	h	4.50	−896.311764	5.65	h	3.80	−1088.047154	4.04
Chloroform	a	0	−896.315377	0	a	0	−1088.04789	0
	h	4.68	−896.309195	3.88	h	4.22	−1088.04134	4.11
Methanol	a	0	−896.320509	0	a	0	−1088.053226	0
	h	4.51	−896.31154	5.63	h	3.82	−1088.046797	4.03
A.Acid	a	0	−896.316781	0	a	0	−1088.049083	0
	h	4.64	−896.309124	4.80	h	4.13	−1088.042672	4.02

[a] The relative energy from the total energy.
[b] The sum of the electronic and thermal free energy of the geometrically optimized dye structure using DFT calculations.

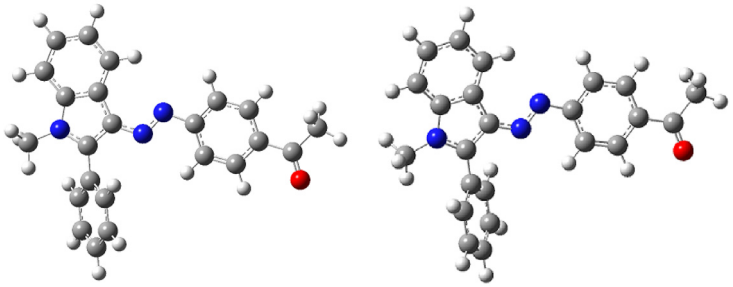

E= -1127.63646170 a.u E= -1127.63646172 a.u.

Fig. 5. Two conformers of dye 4 with the total energy of −1127.63646170 a.u. and −1127.63646172 a.u.

Table 7
Experimental and calculated absorption maxima (λ_{max}) with parenthesized oscillator strength (f) for dyes 1–4.

λ_{max} (nm)								
	DMSO		Methanol		A.Acid		Cloroform	
	Exp.	Calc.	Exp.	Calc.	Exp.	Calc.	Exp.	Calc.
Dye 1	409	410(1.001)	402	408(0.978)	409	407(0.986)	397	409(1.004)
Dye 2	413	417(1.081)	408	415(1.057)	414	414(1.066)	408	416(1.083)
Dye 3	430,530	433(0.797)	422	431(0.778)	421	430(0.791)	417	432(0.808)
Dye 4	417	428(0.932)	408	425(0.909)	414	425(0.919)	413	426(0.936)

Table 8
Experimental and theoretical ^{1}H isotropic chemical shifts (in ppm) for dyes 1–4 calculated using the GIAO-B3LYP with 6-311+G(d,p) basis set.

Atom no.	Dye 1		Dye 2		Atom no.	Dye 3		Dye 4	
	Exp.	Calc.	Exp.	Calc.		Exp.	Calc.	Exp.	Calc.
H3	7.41(d, 1H)	9.00	7.58(d, 1H)	8.93	H3	7.3(m, 2H)	9.14	7.4(m, 2H)	9.17
H4	7.20(m, 2H)	7.65	7.30(m, 2H)	7.69	H4	7.51(m, 2H)	7.70	7.6(d, 2H)	7.79
H5	7.20(m, 2H)	7.66	7.30(m, 2H)	7.73	H5	7.51(m, 2H)	7.71	7.6(d, 2H)	7.76
H6	8.39(d, 1H)	7.67	8.43(d, 1H)	7.76	H6	8.51(d, 1H)	7.87	8.52(d, 1H)	7.81
H9	2.68(s, 3H)	3.03	2.61(s, 3H)	2.99	H10	8.21(d, 2H)	8.23	7.72–7.80(m, 6H)	7.93
H11	7.90(d, 2H)	8.40	7.90(d, 2H)	8.38	H11	7.64(m, 2H)	8.00	7.72–7.80(m, 6H)	8.04
H12	8.11(d, 2H)	8.35	8.10(d, 2H)	8.36	H12	7.3(m, 2H)	7.93	7.40(m, 2H)	8.03
H14	8.11(d, 2H)	8.59	8.10(d, 2H)	8.63	H13	7.64(m, 2H)	7.91	7.72–7.80(m, 6H)	8.03
H15	7.90(d, 2H)	8.37	7.90(d, 2H)	8.29	H14	8.21(d, 2H)	8.70	7.72–7.80(m, 6H)	8.32
H17	2.80(s, 3H)	2.00	2.80(s, 3H)	2.04	H16	7.90(d, 2H)	8.16	7.72–7.80(m, 6H)	7.86
H17	2.80(s, 3H)	3.06	2.80(s, 3H)	3.00	H17	8.12(d, 2H)	8.55	8.08(d, 2H)	8.48
H17	2.80(s, 3H)	3.06	2.80(s, 3H)	3.00	H19	8.12(d, 2H)	8.51	8.08(d, 2H)	8.43
N—R	12.20(brs, NH indole)	8.41	3.81(s, 3H, —NCH_3)	3.89	H20	7.90(d, 2H)	8.45	7.72–7.80(m, 6H)	8.38
					H22	2.65(s, 3H)	2.75	2.62(s, 3H)	2.71
					N—R	12.52(brs, NH indole)	8.67	3.88(s, 3H, —NCH_3)	3.87

s: singlet d: doublet, m:multiplet, brs: broad singlet.

differences between bond lengths and bond angles whereas the differences between torsion angles are seen for two conformations. The selected values obtained from the optimized geometry with the total energy of −1127.63646170 a.u. and also experimental results are given in Table 3. The selected torsion angle values in the parenthesis are for the other conformation with the energy value −1127.63646172 a.u. and for the other of two crystallographically independent molecules obtained by X-ray crystallography. The torsion angle N1—C8—C10—C15 is −130.9° and 130.9° for two conformations and corresponding X-ray results are −139.3(2)° and 131.8(2)°, respectively. Both of the conformers have planar structure. For one of them, C1—N2—N3—C16 torsion angle is −178.96° and for the other 179.0° and corresponding X-ray results are 178.64(19) and 179.8(2), respectively. This value is 178.2° for dye 3.

The differences between the calculated and experimental values are found in the interval 0.001–0.082 Å for dye 2 and 0.001–0.014 Å for dye 4 in bond lengths. The largest difference observed in C8—N1—C7 is 3.6° for dye 2 and in N3—N2—C1 is 2.5° for dye 4.

The calculated N=N distance are obtained as 1.268 Å for both of them. However, X-ray data show that they are double bond character with the value of 1.248(5) Å for dye 2 and 1.275(3) Å for dye 4. It is seen that the experimental and calculated results are good agreement with each other. It is also obtained that the double bond character are seen for dyes 1 and 3 with the values 1.267 Å and 1.268 Å, respectively. It is noted that there is no experimental results of crystal structures parameters for dyes 1 and 3. Therefore, we have calculated the maximum absorption peaks (λ_{max}) at optimized geometries and compared with experimental data.

From the optimized geometry, maximum absorption wavelength (λ_{max}) and corresponding oscillator strengths (f) have been calculated, for each dye, using TD-DFT with the B3LYP/6-311g(d,p) level of theory with DMSO, chloroform, methanol and acetic acid. The theoretical and experimental maximum absorption wavelengths are compared in Table 7. It is obtained that the calcu-

Table 9
The in vitro antibacterial and antifungal activity of synthesized dyes against some microorganisms.

Microorganisms	Diameter of zone (mm)							
	Dye1	Dye2	Dye3	Dye4	SAM	CN	SXT	MCZ
S. aureus	–	–	–	–	20	30	20	–
S. aureus	–	–	–	–	10	20	18	–
S. saprophyticus	–	–	–	–	8	20	16	–
S. saprophyticus	–	–	–	–	10	20	18	–
L. monocytogenes	–	–	–	–	8	10	18	–
L. innocua	–	–	–	–	–	12	16	–
P. aeruginosa	–	–	–	–	–	–	18	–
P. aeruginosa	–	–	–	–	22	24	22	–
P. aeruginosa	–	–	–	–	–	–	18	–
P. aeruginosa	–	–	–	–	–	14	20	–
P. putida	–	–	–	–	–	24	22	–
P. putida	–	–	–	–	–	–	18	–
Esherichia coli	–	–	–	–	–	6	–	–
E. coli	–	–	–	–	–	16	20	–
E. coli	–	–	–	2	–	6	–	–
E. coli	–	–	–	–	–	20	–	–
E. coli	–	–	–	–	–	6	–	–
K. pneumoniae	4	–	–	–	–	16	–	–
K. pneumoniae	2	–	–	–	–	20	18	–
Enterobacter sakazakii	–	–	–	–	–	8	–	–
E. sakazakii	–	–	–	–	–	6	–	–
Candida albicans	–	–	–	6	–	–	–	4
Candida albicans	–	6	4	–	–	–	–	2
Candida tropicalis	2	2	2	2	–	–	–	–

– no activity against to the microorganisms.

lated λ_{max} values and corresponding oscillator strengths values did not change significantly in all the employed solvents and did not correlate with the polarity of the solvent. The calculated values are quite close to the experimental results and the maximum differences between experimental and calculated values are 10 nm for dye 1, 7 nm for dye 2, 14 nm for dye 3 in choloroform and 17 nm for dye 4 in methanol. However, experimentally, the absorption maxima shows little bathocromic shift with increasing dielectric constant for the model compounds (dye 2 and 4). The same trend is observed for dye 2 with the value of 1 nm and for dye 4 with 2 nm in DMSO with respect to the value in chloroform from theoretical calculations. Dyes 1 and 3 exhibit bigger change according to their model compounds. While the experimental results show the difference values between DMSO and chloroform are 12 nm and 13 nm for dyes 1 and 3, respectively, only 1 nm is obtained from the theoretical calculations for each dyes.

Chemical shifts

The calculated ^{1}H NMR chemical shifts for the dyes 1–4 together with the corresponding experimental values with the numbering in Scheme 1 are shown in Table 8. Since experimental ^{1}H chemical shift values were not available for individual hydrogen, the average values for CH_3 hydrogen atoms are presented. As can be seen from Table 8, calculated ^{1}H chemical shift values of the dyes are generally agreement with the experimental data. The ^{1}H NMR spectra measured in DMSO-d_6 for the dyes 1 and 2 showed a singlet peak at 2.68 and 2.61 ppm for indole C—CH_3 respectively. Corresponding calculated values are 3.06 ppm and 2.99 ppm for the dyes 1 and 2, respectively. A broad singlet peak for indole N—H at 12.20 ppm (calc. 8.41 ppm) for dye 1 and a singlet peak appeared at 3.81 ppm (calc. 3.89 ppm) for indole N—CH_3 for dye 2. Similarly, a broad singlet peak for indole N—H at 12.52 ppm (calc. 8.67 ppm) for dye 3 and a singlet peak appeared at 3.88 ppm (calc. 3.87 ppm) for indole N—CH_3 for dye 4.

Generally, N—H proton of hydrazone tautomer appears after 14 ppm values [39]. According to our results, the ^{1}H NMR spectra of dyes 1 and 3 show one signal in DMSO, where the broad signal at 12.20 and 12.52 ppm, respectively, can be assigned to indole N—H which indicates azo tautomeric form.

The antimicrobial activities of the synthesized dyes

The antimicrobial activity of some of the azo dyes has been reported previously [19,41,42].

Recently, it was synthesized different phenylazoindole dyes and screened for their antimicrobial activities on *Bacillus thuringiensis*, *Bacillus subtilis*, *Bacillus megaterium*, *Proteus vulgaris*, *Pseudomonas aeruginosa*, *Staphylococcus aureus*, *Escherichia coli* and *Saccharomyces cerevisiae* [19]. The dyes have showed remarkable activity against *B. megaterium*, *B. subtilis*, *B. thuringiensis* and *S. aureus*, they did not exhibit any activity against *P. vulgaris*. The dyes have showed biological activity on the Gram positive rather than the Gram negative bacteria. However, *Pseudomonas* sp. *E. coli* and *Staphylococcus* sp. showed resistance to most of these compounds, this could be probably due to the R plasmid that is present in them [19].

The antimicrobial activity of seventeen azo disperse dyes against *Bacillus thuringiensis* and *Escherichia coli* are investigated [41]. The novel mordant and disperse azo dyes were synthesized and antimicrobial activity of these dyes against *Escherichia coli*, *Staphylococcus aureus*, *Salmonella typhi*, *Bacillus subtilis* were studied [42]. However, until now, no systematic study has been undertaken to examine the antimicrobial properties of phenylazoindole based dyes. For this reason, in the current investigation, different microorganisms have been chosen and the antimicrobial effect of indole dyes on these microorganisms under in vitro conditions has been studied. The antibacterial and anti-fungal activities of the dyes were determined against 21 bacteria (2 *Staphylococus aureus*, 2 *S. saprophyticus*, 1 *Listeria monocytogenes*, 1 *L. innocua*, 4 *Pseudomonas aeruginosa*, 2 *P. putida*, 5 *Escherichia coli*, 2 *Klebsiella pneumoniae*, 2 *Enterobacter sakazakii*) and three yeast. The data for the antimicrobial tests are summarized in Table 9.

It was generally observed that the dyes were low or no active against test microorganisms. The highest inhibition of growth occurred in dye 2 against *Candida albicans* and dye 4 against *Candida*

albicans as 6 mm. Dyes 2 and 3 showed microbial activity against *Candida albicans* and *Candida tropicalis*. When dye 4 showed microbial activity against *E. coli*, *Candida albicans*, *Candida tropicalis*; dye 1 showed microbial activity against 2 *K. pneumoniae* and *Candida tropicalis*. The all dyes were no activity against 2 *S. aureus*, 2 *S. saprophyticus*, *L. monocytogenes*, *L. innocua*, 4 *P. aeruginosa*, 2 *P. putida*, 4 *Esherichia coli*, 2 *Enterobacter sakazakii* bacteria.

Conclusions

As a result, new series phenylazoindole dyes were synthesized and characterized in this study. The most stable tautomeric form of these dyes were determined easily by using model compounds (dye 2 and 4) in solution and solid state. All spectroscopic data showed that the azo form is predominant for dyes 1 and 3. The experimental data are compared with theoretical values and it was found that the calculation results are in very good agreement with the experimental data. Microorganisms (e. g. bacteria, fungi) have different cell wall structure and plasmids. Plasmids carry genes that may benefit survival of the microorganism (like antibiotic resistance). Dyes using in the research were low and no active against test microorganisms, this could be due to plasmid that is present in bacteria and fungus.

Acknowledgement

The theoretical part of this work is supported by a grant from Gazi University (BAP: 18/2011-06).

References

[1] K. Hunger, Industrial Dyes Chemistry, Properties and Applications, WILEY-VCH Verlag GmbH & Co. KgaA, Weinheim, 2003.
[2] S.C. Catino, R.E. Farris, Azo dyes, in: M. Grayson (Ed.), Concise Encyclopedia of Chemical Technology, John Wiley and Sons, New York, 1985, pp. 142–144.
[3] H. Zollinger, Color Chemistry: Syntheses Properties and Applications of Organic Dyes and Pigments, third ed., Wiley-VCH, 2003.
[4] F. Karcı, N. Ertan, Dyes Pigm. 64 (2005) 243–249.
[5] K. Tanaka, K. Matsuo, A. Nakanishi, Jo H. Shiota, M. Yamaguchi, S. Yoshino, Chem. Pharm. Bull. 32 (1984) 391–399.
[6] A.A. Fadda, H.A. Etmen, F.A. Amer, M. Barghout, K.S. Mohammed, J. Chem. Technol. Biot. 61 (1994) 343–352.
[7] J. Isaad, A. Perwuelz, Tetrahedron Lett. 51 (2010) 5810–5814.
[8] Q. Wang, Y. Long, L. Liangliang, Z. Chuanzheng, X. Zhen, Tetrahedron Lett. 49 (2008) 5087–5089.
[9] J. Wang, C.S. Ha, Tetrahedron 65 (2009) 6959–6964.
[10] H. Bach, K. Anderle, Th. Fuhrmann, J.H. Wendorff, J. Phys. Chem. 100 (1996) 4135–4140.
[11] R.J.H. Clark, R.E. Hester, Spectroscopy of New Materials, Advances in Spectroscopy, Willey & Sons, New York, 1993.
[12] K. Taniike, T. Matsumoto, T. Sato, Y. Ozaki, K. Nakashima, K. Iriyama, J. Phys. Chem. 100 (1996) 15508–15516.
[13] N. Biswas, S. Umapathy, J. Phys. Chem. A 104 (2000) 2734–2745.
[14] I. Willner, S. Rubin, Angew. Chem., Int. Ed. Engl. 35 (1996) 367–385.
[15] M. Ochia, K. Wakabayashi, T. Sugimura, M. Nagao, Mutat. Res., Genet. Toxicol. Environ. Mutagen. 172 (1986) 189–197.
[16] S. Arora, H. Singh Saini, K. Singh, Color. Technol. 123 (2007) 184–190.
[17] S. Arora, H. Singh Saini, K. Singh, Color. Technol. 121 (2005) 298–303.
[18] M. Oimomi, M. Hamada, T. Hara, J. Antibiot. 27 (1974) 987–988.
[19] A. Ozturk, M.I. Abdullah, Sci. Total Environ. 358 (2006) 137–142.
[20] M.R. Yazdanbakhsh, A. Mohammadi, M. Abbasnia, Spectrochim. Acta, Part A: Mol. Biomol. Spectrosc. 77 (2010) 1084–1087.
[21] C. Perez, M. Paul, P. Bazerque, Acta Biol. Med. Exp. 15 (1990) 113–115.
[22] M.J. Frisch, et al. Gaussian 09, Revision A.02. Gaussian, Inc., Wallingford, CT, 2009.
[23] (a) A.D. Becke, J. Chem. Phys. 98 (1993) 5648–5652;
(b) C.T. Lee, W. Yang, R.G. Parr, Phys. Rev. B 37 (1988) 785–789;
(c) P.J. Stephens, F.J. Devlin, C.F. Chabalowski, M.J. Frisch, J. Phys. Chem. 98 (1994) 11623–11627.
[24] R. Ditchfield, Mol. Phys. 27 (1974) 789.
[25] K. Wolinski, J.F. Hinton, P. Pulay, J. Am. Chem. Soc. 112 (1990) 8251.
[26] R.H. Blessing, Acta Crystallogr. A 51 (1995) 33–38.
[27] G.M. Sheldrick, Acta Crystallogr. A 64 (2008) 112–122.
[28] M.A. Salvador, P. Almeida, L.V. Reis, P.F. Santos, Dyes Pigm. 82 (2009) 118–123.
[29] Z. Seferoğlu, T. Hökelek, E. Şahin, N. Ertan, Acta Crystallogr. E 62 (2006) 2108–2110.
[30] Z. Seferoğlu, T. Hökelek, E. Şahin, N. Ertan, Acta Crystallogr. E 62 (2006) 3492–3494.
[31] Z. Seferoğlu, T. Hökelek, E. Şahin, A. Saylam, N. Ertan, Acta Crystallogr. E 62 (2006) 4130–4131.
[32] Z. Seferoğlu, N. Ertan, T. Hökelek, E. Şahin, Dyes Pigm. 77 (2008) 614–625.
[33] Z. Seferoğlu, T. Hökelek, E. Şahin, N. Ertan, Acta Crystallogr. E 62 (2006) 3835–3837.
[34] Z. Seferoğlu, T. Hökelek, E. Şahin, A. Saylam, N. Ertan, Acta Crystallogr. E 62 (2006) 5488–5489.
[35] Z. Seferoğlu, T. Hökelek, E. Şahin, N. Ertan, Acta Crystallogr. E 63 (2007) 148–150.
[36] Z. Seferoğlu, T. Hökelek, E. Şahin, N. Ertan, Acta Crystallogr. E 63 (2007) 351–353.
[37] Z. Seferoğlu, T. Hökelek, E. Şahin, N. Ertan, Acta Crystallogr. E 63 (2007) 568–570.
[38] T. Hökelek, Z. Seferoğlu, E. Şahin, B. Kaynak, Acta Crystallogr. E 63 (2007) 2837–2839.
[39] W. Kuznika, I.V. Kitykb, M.N. Kopylovichc, K.T. Mahmudovc, K. Ozgad, G. Lakshminarayanae, A.J.L. Pombeiroc, Spectrochim. Acta, Part A: Mol. Biomol. Spectrosc. 78 (2011) 1287–1294.
[40] L.J. Farrugia, J. Appl. Crystallogr. 30 (1997) 565.
[41] A.M. Khalil, M.A. Berghot, Monatsh. Chem. 140 (2009) 1371–1379.
[42] B.C. Dixit, H.M. Patel, D.J. Desai, J. Serb. Chem. Soc. 72 (2007) 119–127.